

# Hydrothermal regime analysis of shallow depth of a soil slope during short-term freeze-thaw cycles

Yun Que & Xiaopeng Chen

*College of Civil Engineering, Fuzhou University, Fuzhou, China*

Jinyuan Liu

*Department of Civil Engineering, Ryerson University, Toronto, Canada*



**GEOQuébec**  
2015

*Challenges from North to South*  
*Des défis du Nord au Sud*

## ABSTRACT

This paper presents a study on hydrothermal regime in shallow depth of soil slope during short-term freeze-thaw cycles. The study is conducted by combining both meteorological monitoring and numerical simulation methods and taking a typical short-term frozen zone in Fujian province of China as an example. From December 2013 to February 2014, there were a total of 18 times of freeze-thaw cycles of ambient air temperature: 16 times of two-day, one time of three-day, and one time of six-day cycles. During these short-term freeze-thaw cycles, the air temperature reached the lowest at  $-4.4^{\circ}\text{C}$  and the highest at  $10.8^{\circ}\text{C}$ . The peak of daily radiation ranged from 41 to  $827\text{ W/m}^2$  with an average wind speed from 3.5 to 3.7 m/s. During two-day freeze-thaw cycle of air temperature, the soil freezing time was between 3:00 am and 8:00 am. Based on this study, it is found that air temperature is a major factor in soil freezing, but it is not easy for soil to be frozen in shorter frozen duration.

## RÉSUMÉ

Cet article présente une étude sur le régime hydrothermal de la couche superficielle d'un sol durant de courts cycles de gel-dégel. L'étude est menée en combinant à la fois une surveillance météorologique et une méthode de simulation numérique. Un secteur de la province du Fujian, en Chine, qui présente de courts cycles de gel-dégel typiques est cité en exemple. De décembre 2013 à février 2014, un total de 18 cycles de gel-dégel de la température de l'air s'est produit, dont 16 de deux jours, un de trois jours et un de six jours. Au cours de ces courts cycles de gel-dégel, la plus basse température de l'air enregistrée était de  $-4.4^{\circ}\text{C}$  et la plus élevée était de  $10.8^{\circ}\text{C}$ . Le pic de rayonnement quotidien a été mesuré entre 41 et  $827\text{ W/m}^2$  avec une vitesse moyenne du vent variant entre 3.5 et 3.7 m/s. Au cours d'un cycle de gel-dégel basé sur la température de l'air d'une durée de 2 jours, le sol était gelé entre 3:00 et 8:00. Même si la température de l'air est un facteur majeur dans le gel du sol, le gel de celui-ci est difficile lorsque la durée de la température sous le point de congélation est courte.

## 1 INTRODUCTION

In China, there are about 1.9 million  $\text{km}^2$  of short-term frozen zones, which account for about 19 percent of the total land area of China (Xu et al. 2010). Short-term frozen soil which the frozen duration of soil is from several hours to several days has the characteristics of a high frequency of short-term freeze-thaw cycle and high moisture content under the condition of snow infiltration. The field investigation shows that instability occurs frequently in the shallow layer of residual soil slopes. For example, there are a total of 255 geologic hazardous spots due to short-term freeze-thaw cycles in Nanping city, Fujian province of China, as shown in Figure 1.

Based on the above reasons, the frozen depth of soil, geological disaster type, and the freeze-thaw process in short-term frozen zone are not identical with the permafrost and seasonal frozen soil (Miao et al. 2012). In January 2008, there were a total of 3106 landslides and other geological disasters which were induced by the high strength snow and snow melting reported in Southern China. The main reason for the disasters was due to the geological problems induced by the climate of the south, due to short-time frozen soil zones (Li et al.

2010). Wang et al. (2012) analyzed geographical distributions, frozen level and harmfulness of the southern short-term frozen soil in China. Guo et al. (2012) had analyzed the thermal physical properties and strength characteristics under extreme snow conditions in the southern short-term frozen zone of China. Wang et al. (2011) had analyzed attenuation law of the shear strength index of southern short-term frozen soil which is the typical silty clay in Xianning city, Hubei province of China. Wu et al. (2010) had analyzed the frost-heaving and thawing-settlement variation characteristics of southern short-term frozen soil which is typical reshape clay in Chengdu city, Sichuan province of China. All these results focused on the physical and mechanical parameters, characteristics of short-term frozen soil, but there is limited info on the frozen depth and hydrothermal regime of shallow layer of slope during the frozen-thaw process. To address these issues, this paper takes a typical short-term frozen zone in Fujian province of China as an example, and a hydrothermal regime on shallow layer of soil slope in short-term freeze-thaw cycles is analyzed based on the combination of meteorological monitoring method and numerical simulation.



Fig.1 A typical slope failure due to freeze-thaw cycles in Fujian province

## 2 TYPICAL CLIMATE CHARACTERISTICS AT SHORT-FROZEN ZONE

### 2.1 Field Meteorological Monitoring

The field monitoring spot located at Nanping city, Fujian, China, as shown in Figure 2. Meteorological data is obtained by automatic meteorological monitoring station, shown in Figure 3. The automatic meteorological monitoring station contains air temperature sensor, atmospheric humidity sensor, global solar radiation sensor, wind velocity sensors, etc. The monitoring period is from December 1, 2013 to February 28, 2014.

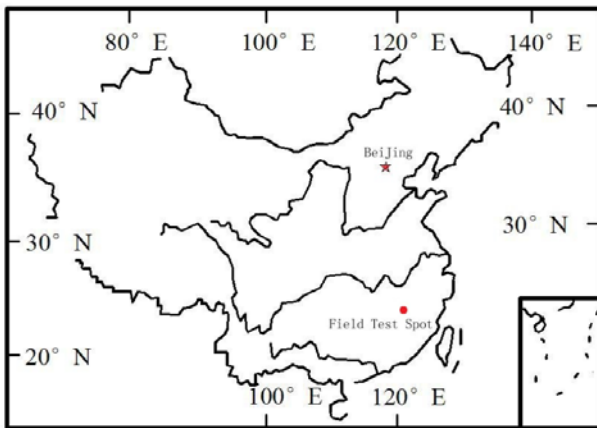


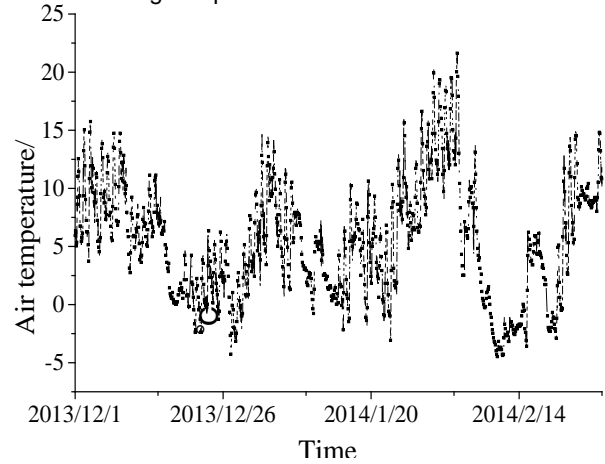
Fig.2 Field test spot



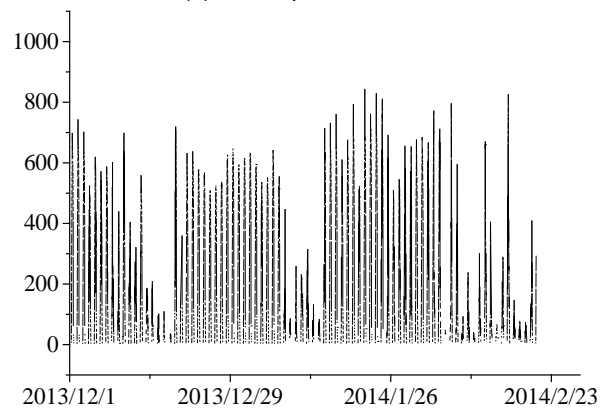
Fig.3 Automatic meteorological monitoring station

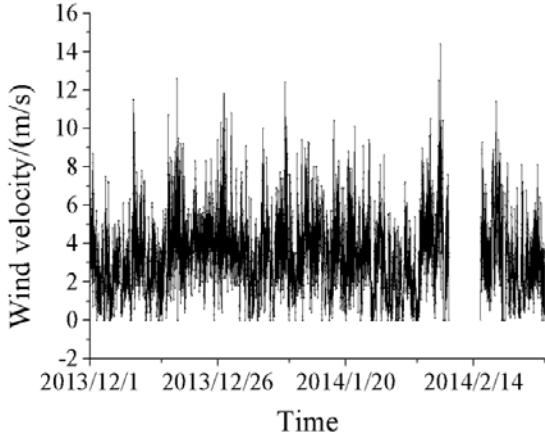
### 2.2 Analysis of Monitoring Results

Because wind velocity sensor was out of order from February 9 to 14, 2014, the data of wind velocity was not collected during this period.



(a) air temperature





(d) wind velocity  
Fig.4 Results of field monitoring

The climate characteristics of short-term frozen zone through the field monitoring resulting in Figure 4 can be described as:

1. The freeze period lasts about three months: December, January and February. There are a total of 18 times of freeze-thaw cycles of air temperature: 16 times of two-day, one time of three-day, and one time of six-day cycles.

2. During the short-term freeze-thaw cycles of air temperature, the minimum and maximum air temperature that can be reached are  $-4.4^{\circ}\text{C}$  and  $10.8^{\circ}\text{C}$ , respectively. The maximum diurnal temperature range can reach  $13.2^{\circ}\text{C}$ . The daily maximum temperature is between 1:00 pm and 3:00 pm and daily minimum temperature is between 5:00am and 7:00am.

3. During the freeze-thaw cycles of air temperature, the peak of daily radiation ranges from 41 to  $827\text{ W/m}^2$ . Time period of solar radiation is at between 7:00 am and 5:00 pm. According to the range of solar radiation from HIPERPAV II (Zhu. 1999), most weather conditions are cloudy and overcast sky in the freeze-thaw cycles air temperatures. Most of the solar radiation is zero when the air temperature is below  $0^{\circ}\text{C}$ . However, there is the coexistence phenomenon of solar radiation and air temperature which is below  $0^{\circ}\text{C}$ . It is also worth noting that during the daytime, the surface layer of the slope will be frozen even in the daytime.

4. During the freeze-thaw cycles of air temperature, the average atmospheric humidity in December and January is about 30%, and the atmospheric humidity in February is over 75%. The atmospheric humidity was correlated with air temperature. The air temperature decreases with the increase of atmospheric humidity.

5. During the short-term freeze-thaw cycle of air temperature, the average wind speed is between 3.5 and 3.7m/s, and the peak of wind speed can reach 14.4 m/s.

### 3 HYDROTHERMAL COUPLING MODEL AND PROGRAMMING

#### 3.1 Hydrothermal Coupling Model

Hydrothermal coupling mode (Harlan 1973) can be described by:

$$\begin{cases} \frac{\partial \theta}{\partial t} + \frac{\rho_i \partial \theta_i}{\rho_i \partial t} = D(\theta) \left( \frac{\partial^2 \theta}{\partial x^2} + \frac{\partial^2 \theta}{\partial y^2} \right) + \frac{\partial K(\theta)}{\partial y} & (1) \\ C \frac{\partial T}{\partial t} - L_f \rho_i \frac{\partial \theta_i}{\partial t} = \lambda \left( \frac{\partial^2 T}{\partial x^2} + \frac{\partial^2 T}{\partial y^2} \right) \end{cases}$$

Where  $\theta$  represents moisture content;  $\theta_i$  represents ice content;  $D(\theta)$  represents water diffusivity,  $\text{cm}^2/\text{s}$ ;  $K(\theta)$  represents transmissibility,  $\text{cm}^2/\text{s}$ ;  $\rho_i$  represents ice density,  $\text{kg}/\text{m}^3$ ;  $\rho$  represents water density,  $\text{kg}/\text{m}^3$ ;  $C$  is heat capacity,  $\text{J}/(\text{g}\cdot\text{K})$ ;  $\lambda$  is thermal conductivity,  $\text{J}/(\text{g}\cdot\text{K})$ ;  $L_f$  is latent heat,  $\text{kJ}/\text{kg}$ ;  $T$  represents the temperature,  $^{\circ}\text{C}$ ;  $t$  represents time, s.

#### 3.2 Equation Solution and Programming

The finite difference model is adopted to solve the hydrothermal coupling model based on Alternating direction implicit method, as shown in Figure 5. The length and height of the numerical model is 7.5 m and 5m, respectively. According to its basic ideology, the analysis is conducted using MATLAB.



Fig.5 Finite difference model(unit:m)

#### 3.3 Boundary Conditions

The boundary conditions include evaporation, solar radiation, net radiation, convective heat transfer, latent heat of evaporation.

Evaporation intensity model (Denisov 2010, Campbell 1974) can be described by:

$$E = \frac{\rho_{vs} - \rho_{va}}{r_v} \quad (2)$$

Where  $E$  is the evaporation intensity,  $\text{mm}/\text{d}$ ;  $\rho_{vs}$  represents the surface vapour density,  $\text{kg}/\text{m}^3$ ;  $\rho_{va}$  represents air vapour density,  $\text{kg}/\text{m}^3$ ;  $r_v$  is drag coefficient.

Thermal boundary is consisted of four parts: latent heat of evaporation, total solar radiation, net radiation and convection heat transfer.

The latent heat of evaporation model (Bristow et al. 1996) can be described by:

$$Q = LE \quad (3)$$

Where  $Q$  is latent heat of evaporation,  $\text{w}/\text{m}$ ;  $T_s$  is soil surface temperature,  $^{\circ}\text{C}$ ;  $L = 2.49463 \times 10^9 - 2.247 \times 10^6 T_s$ .

The solar radiation model (Zhu 1996) can be described by:

$$q_s = \alpha_s \cdot I_f \cdot q_{solar} \quad (4)$$

Where  $q_s$  is absorption heat flux of solar radiation,  $W/m^2$ ;  $\alpha_s$  is the absorption rate of solar radiation;  $I_f$  is the radiation intensity coefficient;  $q_{solar}$  is the peak of solar radiation,  $w/m^2$ .

The net radiation abides by the Stefan-Boltzmann Law (Mu 1987, Zheng 2002). It can be described by:

$$\text{Frozen soil: } L_{sp} = \varepsilon_{sp}(L_a - \sigma T_K^4) \quad (5)$$

$$\text{Unfrozen soil: } L_s = \varepsilon_s(L_a - \sigma T_K^4) \quad (6)$$

Where  $L_{sp}$  represents the net long radiation of frozen soil,  $W/m^2$ ;  $L_s$  represents the net long radiation of unfrozen soil,  $W/m^2$ ;  $T_k$  is the absolute temperature, °C;  $\varepsilon_{\infty}$  is the thermal radiation factor,  $\varepsilon_{\infty}=0.65$ (frozen soil),  $\varepsilon_{\infty}=0.8$ (unfrozen soil);  $\sigma$  is a constant value,  $W/m^2 \cdot K^4$ ,  $\sigma=5.6697 \times 10^{-8} W/m^2 \cdot K^4$ .

The convective heat transfer (Chen 2012) can be described by:

$$q = h_c(T_s - T_a) \quad (7)$$

Where  $q$  is convective heat transfer,  $J/(m^2 \cdot s)$ ;  $h_c$  is the convective heat transfer factor,  $J/(m^2 \cdot s \cdot ^\circ C)$ ;  $T_a$

represents air temperature, °C;  $T_s$  represents soil temperature, °C.

The convective heat transfer factor (Chen 2012) can be described by:

$$h_c = 3.727A(0.9(T_s + T_a) + 32)^{-0.181} |T_s - T_a|^{0.266} \sqrt{1 + 2.857u} \quad (8)$$

Where  $A$  is a constant value,  $A=1.79$ (the soil temperature is higher than air temperature),  $A=0.89$  (the air temperature is higher than soil temperature);  $u$  is wind speed,  $m/s$ .

Temperature daily variation model proposed by Yan (1984) can be described by:

$$T_a = T_1 + T_2[0.96 \sin \omega(t - t_0) + 0.14 \sin 2\omega(t - t_0)] \quad (9)$$

Where  $T_a$  is the air temperature, °C;  $T_1$  is the daily mean temperature, °C;  $T_2$  is amplitude of daily air temperature, °C;  $t_0$  is the initial phase,  $h$ ,  $t_0=9$ ;  $\omega$  is the angular frequency,  $\omega=2\pi/24(rad)$ .

### 3.4 Calculation Parameters

The physical and mechanical parameters of soil sample are shown in Table 1.

Table 1 Physical and mechanical parameters of soil sample

dry density $r_d$ ( $g \cdot cm^{-3}$ )	liquid limit $W_L$ (%)	plastic limit $W_P$ (%)	Plastic index $I_P$ (%)	Saturated conductivity $K_S \times 10^{-5}$ ( $cm \cdot s^{-1}$ )	Non Uniform coefficient $C_u$	Curvature coefficient $C_c$
1.78	25.85	38.57	12.72	5.56	73	0.877

The specific heat capacity of unfrozen and frozen framework grain are 0.84 and 0.77  $kJ/(kg \cdot K)$ , respectively. The specific heat capacity of water and ice are 4.12 and 2.09  $kJ/(kg \cdot K)$ , respectively.

The thermal conductivity of frozen soil (Mao et al. 2006) can be described by:

$$\lambda_f = 0.104 \times 10^{-3} r_d^{0.921} + 3.72 \times 10^{-5} r_d \theta \quad (10)$$

Where  $\lambda_f$  is thermal conductivity of frozen soil,  $w/cm \cdot k$ ;  $r_d$  is the dry density of soil,  $kg/m^3$ .

The thermal conductivity of unfrozen soil (Mao et al. 2006) can be described by:

$$\lambda_u = 0.408 \times 10^{-3} r_d^{0.945} + 1.72 \times 10^{-5} r_d \theta \quad (11)$$

Where  $\lambda_u$  is thermal conductivity of unfrozen soil,  $w/cm \cdot k$ .

The latent heat (Zheng et al. 2002) can be described by:

$$Q = L \rho_d (w - w_u) \quad (12)$$

Where  $Q$  is latent heat,  $kJ/m^3$ ;  $\rho_d$  is dry density,  $kg/m^3$ ;  $w$  is total water content rate;  $w_u$  is unfrozen water content rate,  $kJ/m^3$ ;  $L$  is water freeze-thaw latent heat,  $kJ/kg$ ,  $L=334.56 kJ/kg$ .

The soil-water characteristic curve is fitted by the Van Genuchten model. The Van Genuchten Model (Van 1980) can be described by:

$$\theta(H) = \begin{cases} \theta_r + \frac{\theta_s - \theta_r}{\left[1 + |\alpha H|^n\right]^m} & H < 0 \\ \theta_s & H \geq 0 \end{cases} \quad (13)$$

Where  $\theta$  is soil water content rate;  $\theta_r$  is residual moisture content;  $\theta_s=0.38$ ;  $H$  is the soil negative pressure,  $kPa$ ;  $\alpha$ ,  $n$  and  $m$  are the fitting parameters,  $\alpha=0.0163$ ,  $n=1.7445$ ,  $m=0.4268$ .

The fitted result of Van Genuchten model is shown in Figure 6.

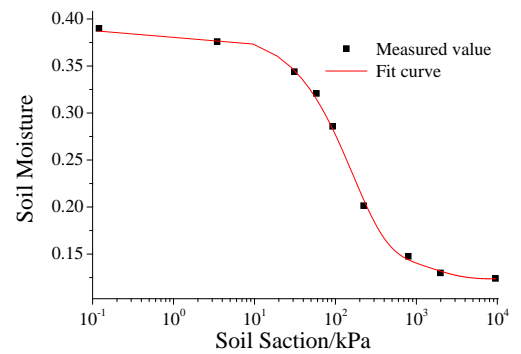


Fig.6 Soil-water characteristic curve

The transmissibility of unfrozen soil is given by Mao et al. (2006) as:

$$K(\theta) = K_s S_e^{1/2} [1 - (1 - S_e^{1/m})^m]^2 \quad (14)$$

Where  $K(\theta)$  is transmissibility of unfrozen soil,  $cm^2/s$ ;  $S_e$  is the effective saturation,  $cm^2/s$ ;  $K_s$  is the saturated hydraulic conductivity,  $cm/s$ ;  $I = 10^{10\theta}$ .

The transmissibility of frozen soil (Mao et al. 2006) can be described by:

$$K_i(\theta) = K(\theta) / I \quad (15)$$

Where  $K_i(\theta)$  is transmissibility of frozen soil,  $m/h$ .

The moisture diffusion coefficient of unfrozen soil (Mao et al. 2006) can be described by:

$$D(S_e) = \frac{(1-m)K_s S_e^{1/2-1/m}}{\alpha m(\theta_s - \theta_r)} [(1 - S_e^{1/m})^{-m} + (1 - S_e^{1/m})^m - 2] \quad (16)$$

Where  $D(S_e)$  is the moisture diffusion coefficient of unfrozen soil,  $cm^2/s$ .

The moisture diffusion coefficient of frozen soil (Mao et al. 2006) can be described by:

$$D_i(\theta) = D(\theta) / I \quad (17)$$

Where  $D_i(\theta)$  represents the moisture diffusion coefficient of frozen soil,  $cm^2/s$ ;  $D(\theta)$  represents the moisture diffusion coefficient of unfrozen soil,  $cm^2/s$ .

### 3.5 Initial Conditions

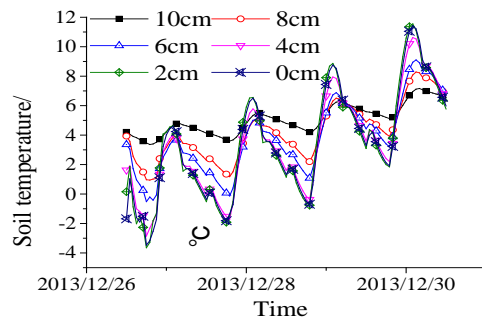
The initial water content is 0.25. The frozen temperature of soil is about  $-1.9^\circ C$  when the water content of soil is 0.25. The initial temperature distribution of slope is determined by the field test results (Chen 2014):

$$T(x, y) = 0.6986 + 96.09x - 1.201y - 500.7x^2 + 3.432xy + 0.1489y^2 + 799.6x^3 + 1.112x^2y - 0.5532xy^2 \quad (18)$$

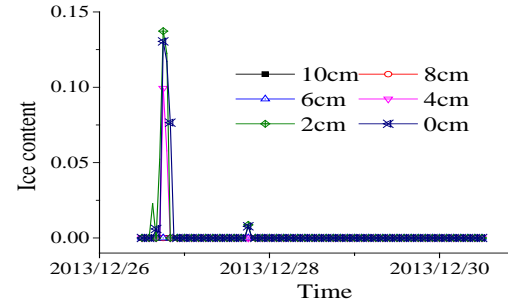
Where  $x$  represents the horizontal depth,  $m$ ;  $y$  represents vertical height,  $m$ .

## 4 NUMERICAL SIMULATION RESULTS

A total of 6 times of freeze-thaw cycles of air temperature was measured in December 2013. In order to calculate the hydrothermal regime of shallow depth of a soil slope, the climate data from December 26, 2013 to December 30, 2013 were selected as the typically freeze-thaw cycle of air temperature. The calculation results for different depths are shown in Figure 7.



(a) soil temperature



(b) ice content

Fig.7 Hydrothermal regime of shallow soil slope from December 26 to 30, 2013

A total of 8 two-day freeze-thaw cycles of air temperature were measured from December 26, 2013 to December 30, 2013. The minimum air temperature is  $-4.4^\circ C$ ,  $-3.1^\circ C$  and  $-2.1^\circ C$  respectively, and freezing time of soil is 7 h, 12 h, and 1 h, respectively. There are two freeze-thaw cycle processes in the shallow depth of a soil slope. The first freeze-thaw cycle process occurred from 3:00 am to 8:00 am on December 27, 2013 and the lowest temperature was  $-3.8^\circ C$ . The second freeze-thaw cycle process occurred from 6:00 am to 7:00 am on December 28, 2013 and the lowest temperature was  $-2.0^\circ C$ . The maximum ice content of the shallow depth of slope during these two freeze-thaw cycle processes was about 0.14 and 0.01, respectively and the maximum frozen depth was about 5 cm and 3cm, respectively.

Although the duration of air temperature below the soil frozen temperature on December 28, 2013 was longer than that on December 27, 2013, the minimum soil temperature on December 27, 2013 was  $1.2^\circ C$  lower than that of December 28, 2013. Therefore, the maximum ice content of soil slope on December 27, 2013 was higher than that of December 28 and the frozen depth on December 27, 2013 was deeper than that of December 28.

On December 29, the minimum air temperature was  $-2.2^\circ C$  and the minimum soil temperature was only  $-1.7^\circ C$ . The soil was not frozen because the minimum soil temperature was higher than the soil frozen temperature.

Therefore, air temperature is a major factor in soil freezing, but it is not easy for soil to be frozen in shorter frozen durations.

## 5 CONCLUSIONS

This paper presents a study on hydrothermal regime in shallow depth on a soil slope during short-term freeze-thaw cycles. Based on this study, the following conclusions can be made.

1. Based on measurement from December 2013 to February 2014, there was a total of 18 times of freeze-thaw cycles of air temperatures: 16 times of two-days, one time of three-days, and one time of six-days cycles.
2. During the short-term freeze-thaw cycles of air temperature, the minimum and maximum air

temperatures reached were  $-4.4\text{ }^{\circ}\text{C}$  and  $10.8\text{ }^{\circ}\text{C}$ , respectively. The maximum temperature range reached was  $13.2\text{ }^{\circ}\text{C}$ . The peak daily radiation ranged from 41 to  $827\text{ W/m}^2$  and the average wind speed was between 3.5 and 3.7m/s. Most weather conditions were cloudy and overcast during these freeze-thaw cycles. The atmospheric humidity was correlated with air temperature. The air temperature decreases with the increase of atmospheric humidity.

3. During two-day freeze-thaw cycles of air temperature, the soil freezing time was between 3:00 am and 8:00 am. Air temperature is a major factor in soil freezing, but it is not easy for soil to be frozen in shorter frozen durations.

#### ACKNOWLEDGEMENTS

This research is sponsored by the National Natural Science Foundation of China (No. 41302215) and Natural Science Foundation of Fujian Province (No. 2014501185).

#### REFERENCES

- Bristow K. L. and Horton R. 1996. Modeling the impact of partial surface mulch on soil heat and water flow. *Theoretical and applied climatology*, 54(1-2): 85-98.
- Campbell G. S. 1974. A simple method for determining unsaturated conductivity from moisture retention data. *Soil science*, 117(6): 311-314.
- Chen X. 2013. *Hydro-thermal coupled mechanism of residual soil slope in the short-term frozen soil zone*. Fuzhou University, Fuzhou, Fujian, China.
- Chen Z. 2012. *Research on Temperature and Humidity Coupling Effect on the Granite Eluvial Soil Embankment in Fujian Province*. Fuzhou University, Fuzhou, Fujian, China
- Denisov Y. M, Sergeev A. I., Bezborodov G. A., et al. 2002. Moisture evaporation from bare soils. *Irrigation and Drainage Systems*, 16(3):175-182.
- Guo Q., and Sun Y. 2012. Thermal physical performance and compressive strength characteristics of short-term frozen soil in southern area of China, *Yangtze River*, 43(9):51-54.
- Harlan R. L. 1973. Analysis of Coupled Heat-fluid Transport in Partially Frozen Soil, *Water Resoure*, 9(5):1314-1323.
- Li Y., Chai B., Miao H. 2012. Correlation Analysis between Geological Disasters and Extreme Ice-snow Climate in Southern China. *Safety and Environmental Engineering*, 19(6):22-28.
- Mao X., Wang B., Hu C., et al. 2006. Numerical Analyses of Deformation and Stress Fields in Permafrost Regions. *Journal of Glaciology and Geocryology*. 26(4):16-20.
- Miao H., Yin K., Xing L., et al. 2012. Evolution analysis of loose debris slope under condition of extreme snow hazard. *Rock and Soil Mechanics*, 33(1):147-154.
- Mu S., and Ladanyi B. 1987. Modeling of coupled heat, moisture and stress field in freezing soil. *Cold Regions Science and Technology*, 14(3): 237-246.
- Mu S., and Ladanyi B. 1987. Modeling of coupled heat, moisture and stress field in freezing soil. *Cold Regions Science and Technology*, 14(3): 237-246.
- Van G. M. T. 1980. A closed-form equation for predicting the hydraulic conductivity of unsaturated soils. *Soil Science Society of America Journal*, 44(5): 892-898.
- Wang L., Sun Y., Guo Q., et al. 2012. Characteristics of frozen soil in South China under extreme climatic conditions of snow and ice, *Yangtze River*, 43(9):51-54.
- Wang Y., Liu X., Ai C., et al. 2010. Experimental investigation on shear strength parameters C and  $\psi$  for a temporarily frozen soil in South China, *Engineering Journal of Wuhan University*, 43(2) : 198-202.
- Wu L., Xu Q. and Huang R. 2011. Analysis of freezing-thawing test process of unsaturated clay, *Rock and Soil Mechanics*, 32(4):1025-1028.
- Xu X., Wang J. and ZHANG L. 2010. *Frozen Soil Physics*. Science Press, Beijing, China.
- Yan Z. 1984. Analysis of the Temperature Field in Layered Pavement System. *Journal of Tongji University*, 43: 51-54.
- Zheng X., Fan G., and Xing S. 2002. *Soil Water Transfer in Seasonal Unsaturated Freezing and Thawing Soil*, Geological Publishing House, Beijing, China
- Zhu B. 1999. *Thermal Stresses and Temperature Control of Mass Concrete*. China Electric Power Press, Beijing, China.